搅拌摩擦焊接过程温度场数值模拟

王希靖[1], 韩晓辉[1,2], 郭瑞杰[1], 李 晶[1]
(1. 兰州理工大学 甘肃省有色金属新材料国家重点实验室, 甘肃 兰州 730050;
2. 中国南车集团四方机车车辆股份有限公司, 山东 青岛 266031)

王希靖

摘 要: 在深入考虑搅拌摩擦焊的具体焊接过程后, 提出了简化的热输入模型。利用ANSYS有限元分析程序建立了随热源一起移动的坐标系, 采用分步加载的方法对搅拌摩擦焊过程的温度场进行了模拟。得到了 3mmLY12硬铝合金薄板在整个焊接过程中焊缝区每一时刻的瞬态温度场以及焊缝区各点的焊接热循环曲线, 确立了温度场空间分布和时间变化的规律, 并且通过测量特征点的实际温度验证了计算结果的准确性。

关键词: 数值模拟; 热输入模型; 温度场; 载荷步; ANSYS; 移动坐标系
中图分类号: TG459 文献标识码: A 文章编号: 0253-360X(2005)12-17-04

0 序 言

温度场对焊缝的组织和性能有直接的影响, 温度场的数值模拟是研究焊缝组织、性能、焊接变形和残余应力的基础。目前, 国内对搅拌摩擦焊温度场数值模拟的工作进行不多, 国外研究进展多停留在二维稳态温度场的建立上[1,2]。研究基于移动热源的特点, 根据温度场叠加原理, 采用分步加载的求解方法, 建立了 3mm LY12硬铝合金完整准确的三维瞬态温度场, 加深了对搅拌摩擦焊温度场的认识, 为制定搅拌摩擦焊工艺提供了有利的理论依据。

1 热模型建立

根据文献[3~5]提出的热输入模型, 作者假设搅拌针为没有螺纹的圆柱, 忽略焊接过程中只占极少量的塑性变形功, 提出了简化的热输入模型[7], 摩擦头与工件产热由轴肩和探针与工件的摩擦两部分组成:

轴肩与工件表面摩擦的热输入

$$p_{sh}=\int_{r_{pin}}^{r_{edg}} q_r 2\pi r\,dr, \tag{1}$$

式中: q_r为搅拌针半径为 r时的热流密度。

$$q_r=R_{eL}\pi nr\beta, \tag{2}$$

式中: r为距摩擦头中心轴线的距离, 满足 $r_{pin}\leqslant r\leqslant r_{edg}$, 搅拌针半径 r_{pin}为 3mm, 长度为 2.5mm; 轴肩半径 r_{edg}为 12mm; n为摩擦头旋转速度; R_{eL}为随温度变化的屈服强度, 其值如表 1所示。

表 1 LY12硬铝合金热物理属性参数表

Table 1 Thermo physical parameters of LY12

属性参数	温度 T/℃			
	100	200	300	400
比热容 C/(J·kg^{-1}·℃$^{-1}$)	921	1047	1130	1172
导热系数 λ/(W·m^{-1}·℃$^{-1}$)	134.4	151.2	172.2	176.4
换热系数 α/(W·mm^{-1}·℃$^{-1}$)	45	61	80	106
屈服强度 R_{eL}/MPa	150	120	80	—

搅拌针与工件内部摩擦的热输入:

$$p_{pin}=\beta V_{pin}, \tag{3}$$

式中: V_{pin}为搅拌针的体积; β为单位生热率。

$$\beta=R_{eL}\pi n/30. \tag{4}$$

2 模拟过程

2.1 定义单元类型

由于工件形状规则, 划分网格和计算时不涉及单元变形对计算精度的影响, 所以不必采用具有中间节点的单元, 在此选择 SOLID70 3-D 八节点六面热体单元。每节点有一个温度自由度, 可以承受表面和体积载荷, 满足分析要求。

2.2 网格划分

根据提出的热模型, 温度场沿焊缝呈对称分布, 所以取工件的一半进行研究。为了保证计算的准确

收稿日期: 2004-07-12
基金项目: 甘肃省攻关项目资助(GS012-A52-069)

性而同时又尽可能减少计算量,在划分网格时采用非均匀网格方式,靠近焊缝中心的地方采用最细的网格,而远离焊缝中心的地方采用较稀疏的网格,见图 1。

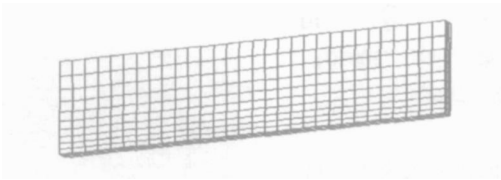

图 1 网格划分形状

Fig. 1 Finite element mesh for temperature field simulation in friction stir welding

2.3 初始条件和边界条件

热物理属性参数如表 1所示,其中 LY12密度为 2 780 kg/m^3,不随温度变化。根据沿焊缝中心对称,对边界条件处理见图 2,把摩擦头肩部与工件接触区域处理成热流密度已知的表面热载荷,搅拌针区域处理成体积热载荷,焊缝中心截面为绝热面,其余各面均处理为对流换热。

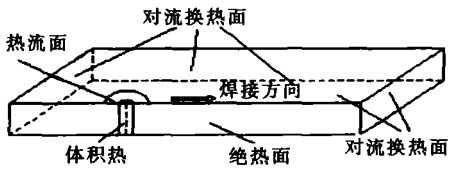

图 2 边界条件与移动载荷

Fig. 2 Boundary condition and moving bad

2.4 求 解

为了更好的模拟焊接瞬态过程,对温度场的模拟采用了移动热源。根据文献[7,8]的观点:连续作用的移动热源周围温度场的数学表达式可以由叠加原理获得。作者对移动热模拟进行如下处理:(1)在很短的时间内假设热源以速度 V匀速移动了 L,所用的时间为 L/N,在这段距离内的移动热源产生的温度场以移动到该小段终点的加热时间 L/N 来近似代替,即向后积分法。当加热时间 L/N很短时,模拟处理可以逼近实际的焊接热源移动问题。(2)沿焊接方向以 L 为长度等分焊缝 N段,在各段的后点依次加载热源各 L/N时间,当下一个点加载开始时,消除上一点所加的热流密度和体积热,上一次加载所得的温度场为下一次加载的初始条件。每次加载为一个载荷步,如此依次在各点进行短时瞬态分析,即可实现对移动焊接瞬态温度场的全程模拟。这一过程可通过 ANSYS有限元分析软件中的参数设计语言 APDL编程循环来实现。

3 模拟结果与分析

针对 3 mm LY12硬铝合金薄板对接焊,取其中的一种焊接参数进行模拟:转速 1 053 r/min,焊接速度 144.4 mm/min,经能量检测装置得到焊接过程准稳态时的扭矩为 29.6 N·m,平均功率为 3 267 W[9]。

3.1 不同时刻的温度等值线图

为了解预热时间对温度的影响,设定了较长的预热时间为 26 s,焊接过程从距离焊接边 30 mm 的地方开始。显示第 26 s、45 s、63.5 s、85 s时工件上表面温度分布,见图 3。随着焊接过程的推移,温度较高的区域在逐渐扩大,而且最高温度区一直跟随摩擦头向前移动;摩擦头前方温度低,后方温度相对较高;摩擦头前方、越靠近摩擦头的区域温度梯度越大,而后方温度变化较为平缓,摩擦头两侧为中等梯度;表面的等温线为封闭的椭圆形,在摩擦头前方密集,后方稀疏。

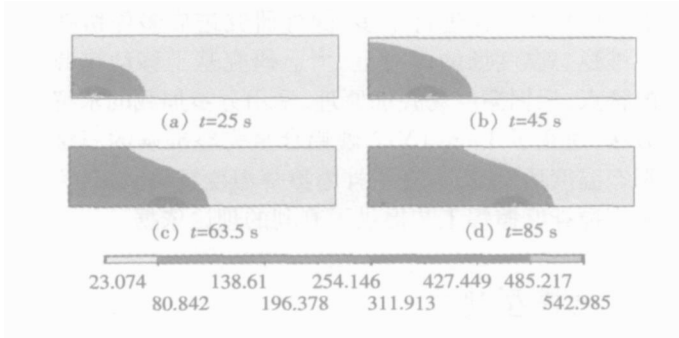

图 3 不同时刻的温度等值线分布图

Fig. 3 Calculated isothermals at different times

3.2 各个特征点的热循环曲线

为了解焊接过程中,即准稳态时焊缝接头的温度变化情况,在板厚中心层上任取距离焊缝中心 6 mm,距离工件开始焊接边分别为 40mm、70mm、100 mm、140 mm、180mm 等五个点,显示其温度历程见图 4。不同横截面的接头经历温度变化过程基本相同,不随位置的变化而改变。图 4中第一条曲线峰值温度较高,是由于摩擦头在此区域停留时间较长;其余各曲线峰值温度一直在缓慢下降,是由于预热时间过长,减少了摩擦头运动的阻力,降低了摩擦产热。图 4中第三条温度曲线最平滑,是因为计算过程中当摩擦头到达距离开始焊接边 140 mm 附近

时，即快到达实际检测温度的截面时，为了使重点研究的区域计算结果更加准确，采用了最小的载荷步。

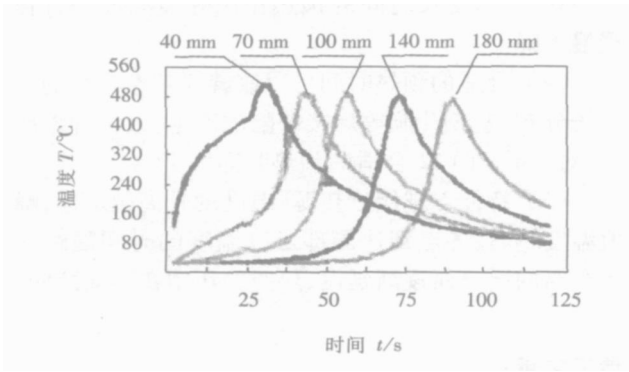

图 4　不同位置的热循环曲线

Fig. 4　Thermal cycling curves at different positions

表 2列出图 4中五条曲线的温度最大最小值，可以看出第一条曲线由于摩擦头停留预热作用，峰值温度较高为 513.9 ℃；其余曲线峰值温度基本不变，保持在 480 ℃左右。

表 2　图 4中各曲线的温度最大值和最小值

Table 2　Maximum and Minimum of temperature curves

	类型	编号	温度最小值 T_1 /℃	时间 t/s	温度最大值 T_2 /℃	时间 t/s
2	节点	10278	75.21	120.0	513.9	32.00
3	节点	11358	25.72	1.733	483.2	44.00
4	节点	12438	23.08	1.733	481.7	56.00
5	节点	13878	23.00	1.733	476.3	73.00
6	节点	15318	23.00	1.733	475.8	90.00

从图 4看出，第一条曲线的变化规律明显不同于其余四条曲线，说明了预热阶段和准稳态阶段热输入对温度影响的差异：热源静止时温度上升变化剧烈，而在热源移动时由于前期的预热作用，温度变化比较缓慢；距静止热源越近的地方，受到的影响越大。

3.3　热源预热作用分析

为深入分析焊接开始阶段的温度变化情况，在距离焊缝中心同样 6 mm 处，选择距离焊接开始边分别为 20mm、30mm、40 mm、60mm、70 mm 的五个点，绘制温度变化过程见图 5。其中静止热源作用在 30mm处，对应于图中温度峰值最高的那条曲线（即第二条曲线），从图 5可以发现：在前 26 s内，温度上升规律相似；在 30 mm 前，温度经历了快速上升，然后逐渐缓降，与第二条曲线相似；距离 30 mm 后越远，温度变化受静止热源的预热作用越小，而是由移动热源引起的温度平滑上升或下降。

为了保证焊接接头在开始阶段与中间过程中温度变化相互一致，需要确定合适的预热时间。同时预热还有以下作用：预热不足时，接头会出现孔洞；预热时间过长时，既降低焊接效率，浪费能源，又会产生过热组织。由图 4知准稳态时的温度值为 480 ℃左右，由图 5可得到在焊缝中心截面上，即第二条曲线由于预热到达准稳态温度 480 ℃的时间为 17 s 左右，此时间即为合适的预热时间。

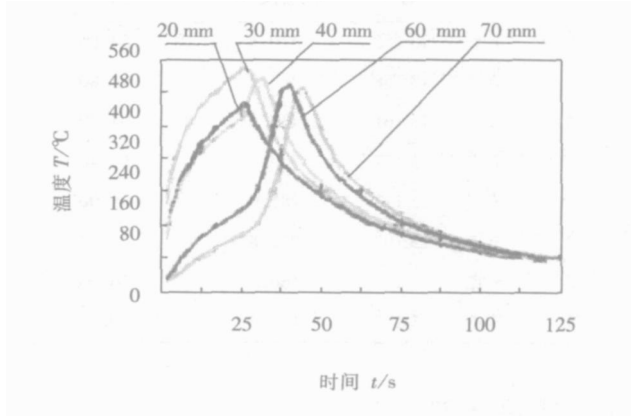

图 5　静止热源附近温度变化过程曲线

Fig. 5　Temperature variation near standing heat source

3.4　同一截面各点温度变化曲线

为观察同一横截面上的温度变化情况，取距离焊接开始边 120 mm 处截面，观察其温度分布。在该截面板厚中心层上取距离焊缝中心分别为 4 mm、6mm、10 mm、14 mm、20 mm、30 mm、40 mm、50 mm 的八个特征点绘制温度历程变化，见图 6。

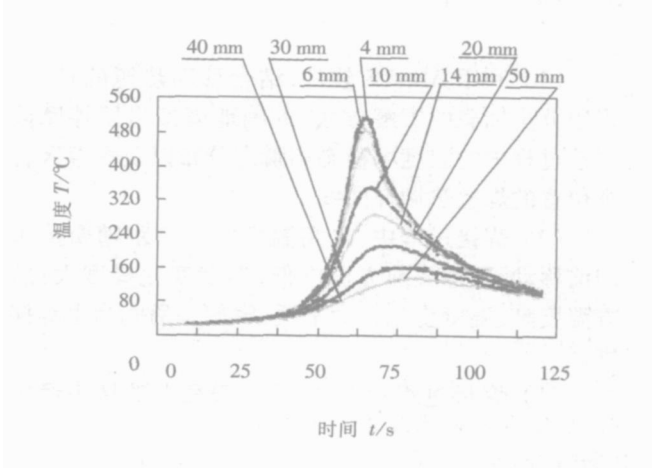

图 6　120 mm 截面上各点温度变化曲线

Fig. 6　Temperature variation at different positions on 120 mm cross section

可以得出:特征点越接近热源,温度的升高越剧烈,最高温度越高;各点到达局部最高温度的时间随着与热源距离的增长而逐渐延迟,说明热源的作用在逐渐减弱。

各曲线峰值温度及其对应时间见表 3,可以根据局部峰值温度确立焊缝区晶粒经历的温度变化及对应的组织分布。

表 3 图 6中各曲线峰值温度

Table 3 Peak temperature at different positions

	类型	编号	峰值温度 T/℃	对应时间 t/s
2	节点	13 155	510.8	64.80
3	节点	13 158	483.2	64.80
4	节点	13 161	439.0	64.80
5	节点	13 167	349.4	66.40
6	节点	13 173	285.0	68.00
7	节点	13 182	212.8	71.00
8	节点	13 191	160.3	76.00
9	节点	13 197	133.6	80.00

4 结果验证

为验证模拟结果是否准确,在焊件上取多个特征点,钻半径为 1 mm的圆柱孔至该点,采用 DR-H电容焊偶仪将镍铬-镍硅热电偶焊合在特征点上,测量特征点的实际温度。结果表明:实验测得的特征点温度过程曲线与模拟曲线相比基本吻合,验证了热模型和模拟处理方法的正确性,具体测温方法见文献[10],部分验证结果见文献[6,10]。

5 结 论

(1)利用 ANSYS软件,结合移动热源的特点,采用分步加载的求解方法,准确地模拟出搅拌摩擦焊接过程中的温度场稳态和瞬态分布以及焊缝区各个位置的焊接热循环曲线。

(2)焊接过程中,最高温度区一直跟随摩擦头向前移动;摩擦头前方温度低,温度变化梯度大;后方温度高,温度变化较为平缓;摩擦头两侧为中等梯度。

(3)焊接过程稳定后,不同横截面的接头经历温度变化过程基本相同,不随位置的变化而改变;距焊缝中心 6 mm处,准稳态时的峰值温度大致保持在 480 ℃,但受长时间的预热作用峰值温度一直在缓慢下降。

(4)合适的预热时间可以改善搅拌摩擦焊的温度场分布,避免孔洞等焊接缺陷的产生,改善焊缝成形,对 3mm LY12合适的预热时间为 17 s。

(5)特征点越接近热源,温度的升高越迅速,峰值温度越高;各点到达局部最高温度的时间随距热源距离的增长而逐渐延迟,热源的作用在逐渐减弱。

参考文献:

[1] Chao Y J, Qi X. Thermal and thermo-mechanical modeling of friction stir welding of alloy 6061-T6[J]. Journal of materials Processing & Manufacturing Science, 1998, (7): 23-27.

[2] Frigaard Q, Grong Q, Midling O T. Modeling of the heat flow phenomena in friction stir welding of aluminum alloys[A]. Proceedings of the Seven International Conference Joints in Aluminum-INALCO'98[C], UK, April 15-17, 1998. 212-214.

[3] Song M, Kovacevic R. Thermal modeling of friction stir welding in a moving coordinate system and its validation[J]. International Journal of Machine Tools Manufacture, 2003, 43(6): 605-615.

[4] Colegrove P. Three dimensional flow and thermal modeling of the friction stir welding process[A]. Proceedings of the second international symposium on friction stir welding[C], Sweden, August 2000. 178-181.

[5] Song M. Numerical and experimental study of the heat transfer process in friction stir welding[J]. Journal of Engineering Manufacture, 2003, 217(1): 73-85.

[6] 王希靖, 郭瑞杰, 阿 荣, 等. 铝合金薄板搅拌摩擦焊温度场模拟[J]. 电焊机, 2004, (增刊): 116-119.

[7] 德国, D. 拉达伊. 焊接热效应[M]. 北京: 机械工业出版社, 1997. 77-81.

[8] 王国强. 实用工程数值模拟技术及其在 ANSYS上的实践[M]. 西安: 西北工业大学出版社, 1999. 95-102.

[9] 王希靖, 陈书锦, 李常锋, 等. 搅拌摩擦焊机控制器的研制[J]. 兰州理工大学学报, 2004, 30(1): 15-18.

[10] 王希靖, 郭瑞杰, 阿 荣, 等. 搅拌摩擦焊接头的温度检测[J]. 电焊机, 2004, 34(1): 22-23.

作者简介:王希靖,男,1956年出生,教授、博导。研究领域为焊接设备及其自动化、搅拌摩擦焊技术以及焊接质量控制,发表论文60余篇,获得部、省级科技进步二等奖 1项,三等奖 7项。

Email: wangxj@lut.cn

MAIN TOPICS, ABSTRACTS & KEY WORDS

Study on arc stability of SACTIG and VPTIG(I) FANG Chen-fu[1,2], CHEN Shu-jun[1], LIU Jia[1], YIN Shu-yan[1], SONG Yong-lun[1], LI Huan[3], HOU Run-shi[4], WEN Yong-ping[2] (1. College of Mechanical Engineering & Applied Electronics Technology, Beijing University of technology, Beijing 100022, China; 2. Provincial Key Laboratory of Advanced Welding Technology, Jiangsu University of Science and Technology, Zhenjiang Jiangsu 212003, China; 3. Material College, Tianjing University, Tianjing 300072, China; 4. Department of Mechnical Engineering, Tsinghua University, Beijing 100084, China). p1 – 5

Abstract: The welding current, arc voltage and shape of SACTIG and VPTIG welding were collected by high-speed camena system and welding arc analyzer. The relation betwenn welding are stabklity and associated parameters during the passing zreo time of SACTIG and VPTIG welding current was analyzed. The studied results indicated that (50Hz) SACTIG arc may go out and reignite during changing polarity. While welding current increase to a threshold the arc will not go out. The higher reignition voltage will caused the longer arc going out, so the arc stability becomes worse. If reignition voltage is equal to arc voltage, the arc will not go out.

Keywords: SACTIG; VPTIG; arc; stability

Thermal fatigue of WC coatings deposited with HVOF WANG Zhi-ping[1], JI Zhao-hui[1], LI Quan-hua[2], LIU Chang-jiang[2] (1. College of Science, Civil Aviation University of China, Tianjin 300300, China; 2. Harbin Turbine Co. ltd, Harbin 150046, China). p6 – 8

Abstract: The thermal shock resistance of the WC coating deposited with HVOF was studied. The results indicated that HVOF coatings after 15 times thermal shock are all perfect without any defects as crack, spalling. In contrast with the coatings deposited with plasma have cracked and spalled completely after 3 times thermal shock. HVOF WC coatings resistance ability to thermal shock is very excellent.

Keywords: HVOF; WC coating; Thermal shock resistance; Thermal shock test

Finite element simulation of thermal stress on the brazed TiC cermet/iron joint FENG Ji-cai, ZHANG Li-xia (National Key Laboratory of Advanced Welding Production Technology, Harbin Institute of Technology, Harbin 150001, China). p9 – 12

Abstract: Maximum value of thermal stress and stress concentration zones of iron/TiC cermet joint brazed at 1 173 K during cooling were studied in this paper. The results show that the shear stress on iron/TiC cermet joint concentrates on the interface tip and the maximum value of the shear stress appears on the Ag-Cu-Zn/TiC cermet interface. The maximum value of tensile stress along TiC cermet undersurface appears on the tips of TiC cermet undersurface, which decreases when the temperature declines. The maximum value of compressive stress along TiC cermet undersurface appears on the center of TiC cermet undersurface, which increases when the temperature declines.

Keywords: Finite element simulation; TiC cermet; iron; brazing

"In-situ" weld-alloying of plasma arc welding of SiCp/Al MMC LEI Yu-cheng, YUAN Wei-jin, ZHU Fei, BAO Xu-dong (Jiangsu University, Zhenjiang Jiangsu 212013, China). p13 – 16

Abstract: Plasma arc welding was used to join SiCp/Al composite and titanium used as alloy filler. Microstructure of the weld is characterized as functions of alloy content. Results show that the acicular harmful phase Al_4C_3 is completely eliminated in the weld of SiCp/Al MMC by "in-situ" weld-alloying of plasma arc welding with titanium. The wetting property was improved between reinforced phase and Al matrix. A stable weld pool, a novel composite material welded joint reinforced by TiN and AlN was produced and welding performance was improved effectively because of the use of titanium. "In-situ" weld-alloying of plasma arc welding is a new promising method for joining of SiCp/Al MMCs.

Keywords: SiCp/Al MMCs; plasma arc welding; "in-situ" weld-alloying; aluminum carbide; titanium nitrogen; aluminum nitrogen

Numerical simulation of temperature field in friction stir welding WANG Xi-jing, HAN Xiao-hui, Guo Rui-jie, LI Jing (State Key Laboratory of Advanced Non-ferrous Metal Materials, Gansu province, Lanzhou University of Technology, Lanzhou 730050, China; 2. Sifang Locomotive & Rolling Stock Ltd., CSR, Qingdao 266031, China). p17 – 20

Abstract: The simplified thermal transfer model was supposed. The moving coordinate system following the heat source was established by using software ANSYS. The method of step-by-step loading was applied in the simulation. The transient temperature field in different positions and thermal cycle curves at different times of 3mm LY12 plate were calculated during the whole welding course. So the temperature field distribution in

space and time was obtained. The calculated results were validated by measuring the actual temperature of characteristic positions.

Keywords: numerical simulation; thermal transfer model; temperature field; load step; ANSYS; moving coordinate system

Wavelet analysis in servo-gun electrode displacement measurement and welding quality control WANG Hua, ZHANG Yan-song, CHEN Guan-long (School of Mechanical Engineering, Shanghai Jiaotong University, Shanghai 200030, China). p21 - 24

Abstract: Electrode displacement curve is an ideal parameter for servo-gun resistance spot welding (RSW) quality control. Electrode displacement curve was separated into trend curve and variation curve by wavelet analysis. Trend curve reflected whole quality of the RSW and variation curve reflected process consistency of the RSW. Electrode displacement curve after wavelet analysis provided good data groundwork for servo-gun RSW quality control.

Keywords: servo gun; electrode displacement; wavelet analysis

Study on micro mechanism for macro/micro manipulator ZHANG Guo-xian, CHEN Qiang, ZHANG Wen-zeng, Tang Xiao-hua (Dept. of Mechanical Engineering, Tsinghua University, Beijing 100084, China). p25 - 28

Abstract: In order to improve the high-speed control capacity of an industrial robot and enlarge its applications in laser welding and cutting, a 3 degree of freedom micro mechanism for macro/micro manipulator was proposed. The micro mechanism structure was analyzed by comparing different kinds of moving forms. Kinematics equation was established, and mechanics characteristic was optimized. The micro mechanism is compact, weighting only 1 kg with a load capacity more than 3 kg and a precision higher than 0.04 mm, meeting the demand of high-precision manufacturing.

Keywords: industrial robot; macro/micro manipulator; micro mechanism; trajectory precision

Diffusion bonding of Ti-6Al-4V to ZQSn10-10 with a copper Inter layer SONG Min-xia[1], ZHAO Xi-hua[1], GUO Wei[1], FENG Ji-cai[2] (1. College of Materials Science and Engineering, Jilin University, Changchun 130022, China; 2. National Key Laboratory of Advanced Welding Production Technology, Harbin Institute of Technology, Harbin 150001, China). p29 - 31, 38

Abstract: The experimental investigation of the diffusion bonding of titanium alloy (Ti-6Al-4V) to Tin bronze (ZQSn10-10) in vacuum was carried out by using pure copper as the transition metal. The microstructure of the joints was studied by SEM, EDS etc. and their mechanical properties were tested by tensile experiments. Experimental results show that using copper as interlayer, it can not only avoid some elements (Sn, Pb etc.) volatilizing but also prevent unwanted elements from diffusion. So the properties of joint can be improved by avoiding more intermetallic compound. The bonding of ZQSn10-10 to copper as interlayer metal is well formed, which intergradation zone can not obviously developed, but the intergradation zone well develop between copper and titanium alloy, which intermetallic compound Cu_3Ti_2 concomitantly appear. The optimum bonding parameters were: bonding temperature T= 850 ℃, bonding pressure P= 10 ~ 15 MPa and bonding time t=30 min. So the strength of the joint without obvious shape change was up to 192 MPa, reaching to about 80% of the strength of base metal ZQSn10-10.

Keywords: titanium alloy; Tin bronze; diffusion bonding; copper interlayer; intermetallic compound

Adaptive fuzzy controller based on variable universe for seam tracking YE Jian-xiong[1], ZHANG Hua[1], YANG Wu-qiang[2] (1. School of Mechanical and Electronic Engineering, Nanchang University, Nanchang 330029, China; 2. School of information Engineering, Nanchang University, Nanchang 330029, China). p32 - 34

Abstract: Aiming at the problem that the precision and the self-adaption are not very well for the pure fuzzy controller in seam tracking of the welding robot, an adaptive fuzzy controller that the universe can be adjusted automatically were designed in this paper. The controller uses the windage and the speed of the windage variation as inputs, and adjusts the universe through the value of windage and windage variation. It can improve the precision and robustness of fuzzy controller. A satisfied effect are gotten by simulation.

Keywords: variable universe; fuzzy controller; self-adaption; simulation

Effect of tool tilt angle on formation and mechanical property of FSW YAN Keng[1], CAO Liang[1], CHEN Hua-bin[2], (1. Provincial key Lab. of Advanced Welding Technology, Jiangsu University of Science and Technology, Zhenjiang, Jiangsu 212003, China; 2. Shanghai Jiaotong University, Shanghai 200030, China). p35 - 38

Abstract: The effect of the tool tilt angle on the characteristics of LF5 aluminum alloy by friction stir welding such as the material flow and mechanical property was introduced. Tunnel defect is observed at 0.5 mm below the tool shoulder as the tilt angle θ is less than 1.5°. Material at lower portion of nugget is deposited. With the increase of θ, defomation and material flow of nugget become more serious, the nugget become wider and the defect disappears gradually. When θ is 2°, kissing bond was found in the upper region through the observation of fracture by SEM. If θ